NASA CR - 111836

INVESTIGATION TO DETERMINE THE FEASIBILITY OF EMPLOYING LASER BEAM HOLOGRAPHY FOR THE DETECTION AND CHARACTERIZATION OF BOND DEFECTS IN COMPOSITE MATERIAL STRUCTURES

by

H.G. Aas

R.K. Erf

J.P. Waters

FEBRUARY 1971

Prepared under Contract No. NAS 1-9926 by

United Aircraft Research Laboratories

UNITED AIRCRAFT CORPORATION

EAST HARTFORD, CONNECTICUT 06108

for

NATIONAL AERONAUTICS AND SPACE ADMINISTRATION

NASA CR-111836

INVESTIGATION TO DETERMINE THE FEASIBILITY OF EMPLOYING LASER BEAM HOLOGRAPHY FOR THE DETECTION AND CHARACTERIZATION OF BOND DEFECTS IN COMPOSITE MATERIAL STRUCTURES

By H. G. Aas, R. K. Erf, and J. P. Waters

Prepared under Contract No. NAS1-9926 by
UNITED AIRCRAFT CORPORATION
East Hartford, Connecticut
for
NATIONAL AERONAUTICS AND SPACE ADMINISTRATION

ABSTRACT

This investigation was directed at determining the feasibility of employing laser beam holography for the detection and characterization of bond defects in composite material structures. With ultrasonic excitation of the composite materials, time-average holography was shown to be capable of: detecting disbonds as small as 0.5 cm. square, determining the size and shape of disbonds and the detection of disbonds under as much as 1.25 mm of composite material bonded to aluminum and titanium. Thermal stressing of the composite materials was shown to be inferior to acoustical stressing. Thermal mapping of the disbonds was shown to be inferior to time-average holography. It was concluded that the technique is an effective one for locating disbonds, but that further development is required to implement a practical inspection system.

INVESTIGATION TO DETERMINE THE FEASIBILITY OF

EMPLOYING LASER BEAM HOLOGRAPHY FOR THE DETECTION AND

CHARACTERIZATION OF BOND DEFECTS IN COMPOSITE MATERIAL STRUCTURES

TABLE OF CONTENTS

INVESTIGATION TO DETERMINE THE FEASIBILITY OF EMPLOYING LASER BEAM HOLOGRAPHY FOR THE DETECTION AND CHARACTERIZATION OF BOND DEFECTS IN COMPOSITE MATERIAL STRUCTURES

By H. G. Aas, R. K. Erf, and J. P. Waters
United Aircraft Corporation

SUMMARY

Presented herein are the results of a study performed over the last six months (1 May 1970 through 1 November 1970) under Contract NAS1-9926, sponsored by the Structures Research Division at the Langley Research Center of the National Aeronautics and Space Administration. The investigation was directed at determining the feasibility of employing laser beam holography for the detection and characterization of bond defects in composite material structures. Relevant to the major objectives of the contract, as called out in the original work statement, the results of the theoretical and experimental investigations with boron-epoxy prepreg composites may be briefly summarized as follows:

1 - Ultrasonic excitation of composite materials, in combination with time-average holography, is capable of:

a- detecting disbonds as small as 0.5 cm square (the smallest area tested);

b- determining the size and shape of most disbonds;

c- detecting disbonds under 1.25 mm of prepreg material (the largest thickness tested); and

d- detecting disbonds in samples with either aluminum or titanium substrates of 0.8 and 1.6 mm thickness (the only substrates tested).

2 - Thermal stressing of composite materials, in combination with real-time holography, is capable of detecting disbonds.

3 - Holography is more effective than thermal mapping, with an infrared scanning camera, of composite materials for detecting disbonds.

In addition it was shown that:

4 - The technique of ultrasonic excitation and holographic observation is equally applicable to graphite composites.

5 - It is possible to acoustically excite the resonant plate modes, necessary for the detection of disbonds, by simple surface contact methods rather than bonded transducers. This considerably facilitates the experimental procedure and suggests application in a practical situation.

The report provides a comprehensive review of the six month investigations directed toward an eventual goal of adapting the holographic method to the rapid inspection of composite aerospace components in a practical (non-laboratory) environment. The discussion, summarizing this feasibility study, has been divided into three general areas:

Section I - Ultrasonic Excitation and Time-Average Holography (including results 1, 4, and 5 enumerated above);

Section II - Thermal Stressing and Real-Time Holography (result 2 enumerated above); and

Section III - Thermal mapping with an IR Scanning Camera (result 3 enumerated above.

INTRODUCTION

The demand for lighter, stronger and more reliable structures has resulted in a new class of materials known as composites. The potential advantages of composite structures has been spectacularly demonstrated by the decrease in weight and the increase in reliability and life expectancy of some aerospace components. The engineering challenge, unregimented by convention, of the apparently limitless possibilities of innovative design is not greater than the challenge to determine the quality of the composite materials; materials which, to a great extent, are too thin, too anisotropic, and too non-uniform for conventional non-destructive testing.

Among the most rapidly developing composite forms is a shell structure formed by aligning high strength fibers such as boron and carbon in an epoxy or metal and bonding or fusing this material to a substrate. While these structures are stronger than conventional, homogeneous materials, current trends in fabrication techniques to realize the new materials tend to introduce numerous bond defects either between individual fiber plies or between the plies and metal substrate. A detailed knowledge of these flaws is required before the reliability of a structure can be evaluated. An important facet in defining the effects of various flaws is the identification of their existence.

This investigation is primarily an empirical approach to establish the requirements for identifying the location and size of a definable unbonded area in a composite structure by the excitation of plate vibrations. The use of plate vibrations for NDT of thin materials has not been practical to date since it requires the analysis of several receiving transducers to determine the location and nature of the changes in the transmitted signal. Interferometric holography immediately records the displacement of the surface with respect to a reference location. Consequently, if a plate vibration is generated whose mode will be changed by the flaw, the location and nature of the flaw can be easily determined from the holographic reconstruction.

Presented in the following section is a description of the interferometric holographic process. This is followed by discussions of the results obtained from a study to determine the feasibility of applying this process to the detection and characterization of bond defects in composite materials. The first and major discussion of these results is concerned with ultrasonic excitation of the test piece and time-average holographic recording. This is followed by a brief section describing the use of thermal stressing and real-time holography as applied to composite material inspection. Finally, experiments with an infrared scanning camera to obtain thermograms of various flawed composite samples are reviewed.

INTERFEROMETRIC HOLOGRAPHY

Holography has permitted the extension of interferometry, classically used to measure small path length differences of optically polished and specularly reflecting flat surfaces to three-dimensional, diffusely reflecting objects, with non-planar surfaces. This radically different concept in interferometry does not require the use of lenses or other image forming devices. Instead, a coherent-optical beam, generated by a laser, is split into two beams, an object beam and a reference beam. The object beam after reflection from the object is superimposed back upon the unaltered reference beam and recorded on a photographic plate. The surface of the test object is then altered through the application of a mild stress and a second recording similar to the first is made on the same photographic plate. The two recorded interference patterns called a double-exposure interferometric hologram, bears no resemblance to the object in two different states of stress but nevertheless contains all the amplitude information about the two wavefronts which had emanated from the object plus additional information about the phase of the wavefronts. These two pieces of information are required in order to gain knowledge about the surface displacement due to the application of the stress.

The creation of an intelligible image from the interferometric hologram is known as the reconstruction process. In this process, the interferometric hologram is illuminated with monochromatic, coherent light; the hologram diffracts this light into two wavefronts, which are essentially indistinguishable from the original waves which had been reflected from the object under the two states of stress and, hence, two three-dimensional images of the object will be formed. Since both images are formed in coherent light and exist at approximately the same location in space, the two reconstructed images will interfere with each other and produce a set of bright and dark interference fringes (in the reconstructed image). The fringes represent contours of equal displacement, along the viewing axis, with each successive fringe representing a displacement of approximately one-half the wavelength of the coherent light source used in the construction process. Thus, using a He-Ne laser (wavelength of 6328 Å), each successive fringe will represent $\sim$0.316 microns of surface displacement. Because of this extreme sensitivity to surface deformation, this technique can be used to gain a meaningful interpretation of the structural integrity of a component by observing the surface movement produced when a mild stressing force interacts with a defect.

In addition to double-exposure holographic interferometry described above, there are two other variations of this method which have been used in the present investigation. Each of the variations possess certain advantages over the others in a particular test situation. These additional techniques include: time-average interferometric holography and real-time interferometric holography.

The time-average technique, which is used most often in the present study for examining the effects of acoustic stressing, consists of making a single holographic recording of a test piece while it is subjected to a cyclic vibratory motion. The technique assumes that the exposure time in recording the hologram is long compared to one period of the vibration cycle. In this manner, the hologram effectively stores an ensemble of images corresponding to the time-average of all positions of the object during its vibration. Consequently, upon reconstruction of the hologram, the interference among the ensemble of images, produces an interference pattern which is weighted toward the deformation extremes of the test piece. Regions having no motion exhibit the greatest intensity and can readily be detected upon inspection of the reconstructed image.

Real-time interferometric holography consists of taking a single holographic exposure of an object in an unstressed state, processing the film and replacing it exactly into the position in which it was recorded. The hologram is then reconstructed using the identical coherent reference light beam which was used in the construction process. The reconstructed image is now superimposed onto the original object which is also illuminated with the same light as when the hologram was taken. Interference fringes can now be seen if the object is slightly stressed. This interferometric comparison between the original state of the object (reconstructed virtual image) and the stressed state of the object is made at the instant of observation. The particular advantage this technique has is that different types of stresses can be applied and observed with a single holographic exposure rather than having to make an interferometric hologram for each.

ULTRASONIC EXCITATION AND TIME-AVERAGE HOLOGRAPHY

The material specified for the present investigation was a composite consisting of several plies of boron-epoxy prepreg bonded to a metal substrate. One test piece with a carbon fiber was tested. In most cases the unbonded area was produced by cutting out an area in one of the plies and inserting a bag fabricated by welding together at the edges two two-mil sheets of stainless steel. Most of the air was removed from between the sheets during the fabrication process. This method had the advantage of producing an area with negligible shear strength and known size, but has the disadvantage of requiring a large excitation force to overcome the bias force of atmospheric pressure.

The excitation of the plate vibrations was, in most cases, accomplished by electrically driving a ferro ceramic transducer which had been bonded to the surface of the test piece. By driving the transducer at the correct frequency, a resonant plate mode can be established in the sample. This method of excitation has the advantage of having a nearly unlimited range of frequencies. Although the amplitude control is limited by the transducer location, this characteristic is not usually disadvantageous since the amplitude of vibration is immediately available from the holographic readout.

In a few cases where larger amplitude vibrations appeared to be required, a transducer was mechanically coupled to the test piece through a solid exponential horn (acoustic transformer). The mechanical advantage of producing large amplitude vibrations with a flexural excitation (bonded transducer) is not greatly different than for the horn coupling; however, the amplitude of vibration for the flexural transducer is limited by the strength of the bond and the optimum placement of the transducer for the desired plate mode. Of additional interest is the fact that horn coupling excitation facilitates the experimental procedure, by eliminating the bonding process, and thereby suggests a practical method for implementation of holographic nondestructive testing.

It had been intuitively expected and previously demonstrated (Ref. 1) that, at least for some conditions, the vibrational amplitude and wavelength in the plate above an unbonded area would be sufficiently different from the remainder of the composite to be readily identified in the reconstruction of a time-averaged interferometric hologram. It was the objective of the present program to determine the reliability of defining unbonded areas by this method and to establish the relationship of wavelength and flaw size.

Analytical Considerations

It was expected that for many cases, at the fundamental mode, an unbonded

area could be considered a clamped circular plate and, as such, its fundamental resonance in Hz is given by[2]:

$$f_o = 0.9342 \frac{h}{a^2}\sqrt{\frac{Y_o}{\rho(1-\sigma^2)}}$$

where h is one-half the plate thickness, a is the plate radius, Y_o is Young's modulus, ρ is the density and σ is Poisson's contraction.

If the material characteristics and thicknesses were such that the resonant frequency of the substrate, the fiber matrix and the bonded composite were equal for the same radius, it would not be possible to detect any mode change. Identifying the composite parameters by the subscript 3, the fiber matrix by the subscript 1, and the substrate by the subscript 2, Young's modulus and the density of the composite may be defined as:

$$Y_{o_3} = \frac{h_1 Y_{o1} + h_2 Y_{o_2}}{h_1 + h_2}$$

and

$$\rho_3 = \frac{h_1 \rho_1 + h_2 \rho_2}{h_1 + h_2}$$

Consequently, the ratio of Y_{o3}/ρ_3 must always lie between Y_{o1}/ρ_1 and Y_{o2}/ρ_2 or be equal to one of them. Since h_3 is the sum of h_1 and h_2, then f_{o_3} must always be different than f_{o1} and/or f_{o2} and the mode pattern of at least one of the individual components will always be different than the composite at f_{o1} and f_{o2}. Furthermore, since the plate wave velocity, as defined below, is proportional to $\sqrt{\omega}$ and the $\sqrt{h}$, where ω is the frequency in radians per second, the differences in the mode pattern will increase as higher order modes are excited.

Also of importance is the minimum size flaw which can be detected. The velocity of propagation of a plate wave v_p is given by[3]:

$$v_p = \sqrt{\frac{2h\omega}{\sqrt{12}}}\sqrt{C_{ext}}$$

where C_{ext} is the extensional velocity of sound. When $2h\omega/\sqrt{12} = C_{ext}$ the plate velocity approaches the extensional velocity of sound and it would be unlikely that a plate vibration could be excited. Since $\omega = 2\pi f$ and $\sqrt{12}$ is nearly equal

to π, the plate and extensional velocities will be equal at the frequency for which the extensional wavelength is approximately equal to twice the plate thickness. Consequently, the minimum dimension of a detectable flaw will be a few times the plate thickness.

Physical Properties and Characteristics of Experimental Components

Flexural Transducers

Ferro ceramic transducers of the lead zirconate titanate Clevite type 4 (PZT-4) were used. Because most high modulus conducting adhesives cure at a moderately high temperature (150°C), and because it was desirable to cure the adhesive under high pressure, which frequently causes some polarization changes in the transducer even though the temperature is below the Curie temperature, great care must be exercised when installing the transducers to minimize the risk of damage. An aluminum foil electrode with an extending tab for electrical connection was bonded to the transducer with a conducting adhesive and the transducer was polarized at room temperature with a voltage of approximately 70 volts per mil of transducer thickness for three hours. The transducer was then bonded to the test piece with a nonconducting epoxy adhesive which cured at 40°C.

Most of the transducers were approximately 1.5 cm. long, 0.5 cm wide and 0.05 cm thick. Larger transducers were used when higher energy was necessary to identify the flaw. In some cases the transducers were installed at the edge of the test piece and a free-free mode was employed; in other cases the transducer was installed a short distance from the edge and the test piece was driven in a cantilevered position with one end of the transducer bearing against the clamp. This technique was more often used since it provided better transducer coupling to the test piece. Driving voltages as high as 210 volts were occasionally required to produce an identifiable mode in the hologram; but generally, 75 to 100 volts provided sufficient excitation.

Exponential Horn Transducer

Piezoelectric transducers are strength limited in tension to strains of approximately 10^{-4}, while in metals the maximum strain can be as high as 10^{-2}. Consequently, a greater driving amplitude than that obtainable by direct bonding of piezoelectric transducers would be desirable. If a sound wave is generated at one end of a transmission line and the area of that line is reduced in such a way that no energy from the wave is reflected away, the particle velocity will vary inversely with the area ratios. Therefore, an aluminum exponential horn was fabricated in which the taper followed the form[4]:

$$S = S_o e^{-\gamma x}$$

where S_o is the initial area and S the area at a distance, x. A γ of 0.7 was chosen to match the horn to the size and resonant frequency of an available transducer. The initial diameter of the horn was 2.5 cm and the final diameter 0.25 cm at a length of 4.9 cm. The half wave resonance of the horn was 48 KHz.

The transducer was PZT-4 with an axial length of 3.75 cm, an outside diameter of 2.5 cm, and a wall thickness of 0.25 cm. The axial resonance of the transducer was 48 KHz when driven across the wall of the cylinder. The transducer was bonded to the aluminum horn and the complete assembly is shown in Fig. 1. The transducer electrodes were placed on the inner and outer surfaces of the cylinder, and the resonant frequency of the assembled transducer was 52 KHz. The transducer is effective as a driver only near its resonant frequency and, therefore, the device can be supported at the mid circumference of the transducer. The results showed that a peak displacement of approximately 10 microns can be obtained at the output of the horn.

Test Piece Material Properties

Boron Fiber

Diameter	10^{-4} meters
Density	2.6×10^3 Kg/m^3
Young's Modulus	38.2×10^{10} N/m^2

Boron Prepreg

Density	2×10^3 Kg/m^3
Young's Modulus	20.6×10^{10} N/m^2
Thickness/ply	1.25×10^{-4} meters

Aluminum

Density	2.8×10^3 Kg/m^3
Young's Modulus	7×10^{10} N/m^2

Titanium

Density	4.5×10^3 Kg/m^3
Young's Modulus	11×10^{10} N/m^2 (estimated)

Flaws

Four types of flaws were evaluated. In the first attempt the programmed, unbonded area was sprayed with a fluorocarbon release agent on the substrate side, and then the prebonded boron prepreg plies were bonded to the substrate

with a low temperature curing adhesive. Plate vibrations indicated no significant change in the mode pattern at the flawed area. The boron prepreg was separated from the substrate and visual observation indicated that sufficient porosity in the release agent existed for the adhesive to penetrate and establish a significant bond strength. Subsequent measurements indicated a shear strength in excess of 7×10^4 N/m^2. Consequently, this technique was not employed for the present investigation; it should, however, offer an attractive method for studying the feasibility of measuring bond strength.

A second type of disbond was fabricated with one mil Mylar sheet. These were made by pressing the Mylar against the substrate with a bolt whose diameter was the size of the desired flaw. This assembly was then clamped together. Adhesive was applied between the substrate and the Mylar around the circumference of the bolt face. A nut was then screwed down the bolt to the substrate to both clamp and smooth the bonded area. This process resulted in a reliable flaw, but subsequent bonding of the prepreg to the substrate with a low temperature curing adhesive resulted in a thick adhesive layer and consequently an inferior test sample. The thick adhesive layer could be eliminated by fabricating the composite in a one-step process after installing the flaw on the substrate, but there was some doubt that the flaw reliability would be equally good. Two of these Mylar samples were tested.

The third flaw type was fabricated by bonding the prepreg to the substrate with a Teflon triangle inserted between the two materials at one edge of the test piece with an extension of one side of the traiangle protruding as a tab. After the adhesive had cured, the Teflon was withdrawn by carefully pulling on the tab.

Most of the tests were conducted with flaws produced by inserting a stainless steel bag in a cut-out area of one of the prepreg plies. Two types of bags, both of which were fabricated from two mil thick stainless steel sheets, were used. One type, supplied by NASA, was made by resistance welding the outer edges of two sheets of stainless steel up to a small tube at one edge of the sheets; the air was then removed and the tube sealed off. The flaw forms were then welded within the enclosed area. A second type of bag was fabricated at UARL by electron beam welding. The stainless steel bag flaws were reliable in that they were of a known size and there was nearly a zero shear and tensile strength in the flaw; they were unrealistic to the extent that a force was required to overcome the bias clamp produced by the pressure differential between the pressure at fabrication and ambient pressure. However, the influence of the pressure differential is calculable. If four plies of prepreg exist above the flaw, the resultant force provided by a one micron peak-to-peak amplitude at 70 KHz is required to overcome the bias force of a good vacuum; if the flaw is under one ply, an amplitude vibration of 4 microns is required at the same frequency.

Composite Sample Descriptions

Of the 22 composite samples fabricated for testing during the course of the contract investigations, 12, fabricated at UARL,produced meaningful results which are presented in the following section.

The specifications for the 12 UARL test pieces providing definitive data are summarized in Table I along with 2 NASA prepared samples which were tested. All of the UARL specimens, which are described in detail in Appendix I, were 5 x 10 cm with the exception of No. 12, which was 10 x 15 cm. Both carbon and boron prepreg on aluminum and titanium substrates were evaluated; photographs, representative of these 4 materials, are presented in Fig. 2.

Experimental Results

The results of the ultrasonic tests for each of the 12 samples fabricated at UARL and one NASA specimen are presented below. Typical holographic reconstructions are reproduced showing the unique mode patterns. Some additional results, visible in the original reconstructions are discussed, but have not been reproduced herein because of thermal distortions and other modes which would probably obscure them in the printing.

Test Piece 1

Although this sample was fabricated with a defective adhesive, the very positive characteristic of the disbond permitted its identification upon ultrasonic excitation and holographic examination. A definite triangular pattern of plate modes at the programmed flaw location, with a driving frequency of 90 KHz, is apparent in the holographic reconstruction of Fig. 3a. Further studies of this test piece using a thermal gradient-holographic technique, described in the following section, were also successful in identifying the flawed area.

Test Piece 2

This sample was fabricated with a different adhesive which provided a good prepreg to substrate bond. The defect was identified at a frequency of 111 KHz, as shown in the holographic reconstruction in Fig. 3b; it appears as the dark spot near the vertical center of the sample with a gray halo of the correct shape and size surrounding the spot.

Test Piece 3

This sample, whose flaws consisted of stainless steel bags placed in cut-outs in the prepreg ply adjacent to the substrate, was assembled by a two step

process. Four prepreg plies were bonded together, and this laminate was bonded to the substrate with a room temperature curing epoxy. It was found that differences in the vibrational modes of the prepreg and substrate became detectable at 30 KHz, suggesting a soft, thick, or acoustically lossy adhesive. It was not possible to excite identifiable mode changes in the area of the programmed flaws under the excitation and boundary conditions employed until a clamp was placed in the vicinity of one of the flaws. This impedance change increased the amplitude sufficiently to identify the mode change as shown in Fig. 4. The effects of clamping both at grazing incidence to the wave propagation (a) and perpendicular incidence to the wave propagation (b) are shown. Excitation was at 126.2 KHz and 126.0 KHz respectively.

Test Piece 4

This sample, prepared in a one-step bonding process, had a 1.6 mm thick substrate, twice that used in the other composite samples. The flaws consisted of three stainless steel bags. The two larger flaws, located in the 1st ply, were easily identifiable by the excitation of vibrational plate modes at several frequencies. Photographs of holographic reconstructions, representative of the results obtained, are presented in Fig. 5. It was not possible to identify the third smaller flaw, located in the 3rd ply, even with the transducer drive excitation on the boron prepreg side; excitation is usually applied on the substrate side.

The fundamental resonance of the plate (one prepreg ply) above this flaw is greater than 50 KHz and, with a plate thickness of 0.125 mm, a peak-to-peak vibrational amplitude of greater than 4 microns would be required to overcome the pressure differential between the flaw and ambient pressure; it was concluded that the flaw was not identified because of insufficient vibrational excitation amplitude.

Test Piece 5

Representative results obtained with this sample are presented in Fig. 6. The mode changes at the Mylar film flaws, particularly the larger one, are quite evident. The smaller one is only visible in the photo at the far right and appears nearer the bottom of the sample, rather than the top, since it is a mirror image of the actual test piece. The stainless steel bag flaw was not identifiable.

Test Piece 6

In order to obtain some evidence of the physical characteristics of a flaw produced by cutting a piece out of a sheet adhesive and using a release agent on the substrate, a sample was made up with a glass substrate. Presented in Fig. 7a

is a photograph of the sample (the horizontal line is a crack in the glass caused by differential expansion) with an enlargement of the lower left corner of the flaw shown in Fig. 7b. The whitest area is the portion sprayed with the release agent, the darkest area is the prepreg material in the absence of adhesive, and the gray area is the adhesive itself. In spite of the fact that the sheet adhesive had been cut out in the area of the release agent, the entire area was penetrated by the adhesive and the gas from the void area had apparently penetrated the adhesive. It is estimated that perhaps 10 percent of the release treated area is bonded and that the point-to-point pinning distance is such that an excitation frequency in excess of 200 KHz would be required to produce any delineating moding.

Test Piece 7

Representative results obtained with this sample are presented in Fig. 8 illustrating applicability of the interferometric holographic technique to composites with a titanium substrate. All of the flaws, including the 0.5 x 0.5 cm square, are apparent at various excitation frequencies as noted in the figure.

Test Piece 8

This particular sample was prepared to evaluate the difference between resistance welding and electron beam welding of the stainless steel bags used as the flaws. Although the stainless steel bags are intended to be identical, the UARL electron-beam welded bag is somewhat thicker at the weld than the 4 mil thickness of the two stainless sheets because of the bead at the seam, while the NASA resistance welded bag is 4 mils thick at the weld. This means that at the seam, the UARL bag is slightly thicker than one prepreg ply. The test piece has not been disassembled so it is not known how the prepreg is distorted by the electron beam welds nor how the prepreg epoxy flows into the voids in the fabrication process, but there does seem to be some difference in the vibrational response of the two types of debonds. Figure 9a shows a mode at the location of the UARL bag at 56.9 KHz while Fig. 9b shows a similar response at the NASA bag location at 50.8 KHz. In both cases, the plate mode resonance was excited by a transducer adjacent to the identified flaw, and the plate was reversed left to right between the two tests such that the identified flaw was near the clamped end (left side of picture). It could be expected that the 10 percent change in frequency accounted for a change in the level of response, but several holograms were made at several frequencies of similar magnitude and, in each case, the flaw produced by the NASA bag had a larger mode pattern. (The broad dark fringes, washing out the right hand side of the picture, were caused by overall plate movement due to heating of the sample by the driving transducer. This is correctable by driving for a short time to allow the sample to reach thermal equilibrium before making the holographic exposure.)

Test Piece 9

This sample was prepared to evaluate the capability of the technique in detecting flaws under a relatively large thickness of prepreg. The 10 plies of prepreg (1.25 mm thick, density of approximately 2 x 10^3 Kg/m^3) provided sufficient mass to permit the identification of mode changes in the vicinity of the unbonded area on the substrate side of the sample as well as on the prepreg side. The unbonded area produced by such a large flaw (2.5 x 2.5 cm stainless steel bag) also permits identifiable modes at relatively low frequencies. Figure 10a shows a one-one mode at 10.8 KHz on the substrate side and Fig. 10b is the same mode on the prepreg side at 15.0 KHz. Figure 10c shows the two-one mode on the prepreg side at 23.8 KHz. Figures 10d and 10e are the modes set up at 29.9 KHz on the substrate side and 29.4 KHz on the prepreg side respectively; the change in the resonant plate mode pattern in the vicinity of the flaw at these frequencies (approximately 30 KHz) indicates that such flaws could also be detected by 30 KHz traveling waves in large composite structures.

Test Piece 10

In order to evaluate this holographic nondestructive testing (HNDT) method for graphite composites, a 5 ply sample of graphite prepreg bonded to titanium was fabricated. As in many of the samples, 3 stainless steel bags of varying size were incorporated in the first ply. The large (1.0 x 1.0 cm) flaw in the center of the sample appeared to slightly alter the symmetrical plate modes as low as 15.9 KHz and to cause substantial changes at 29.6 KHz; but a frequency at which the entire area of the large flaw was well delineated was not found. Figure 11a shows the disruption of the normal mode in the area of the large flaw at 44.8 KHz. As seen in Figs. 11b, c, and d, the flaw on the left side was displaced toward the edge of the sample in the fabrication process; it stands out especially well in Fig. 11b. All three flaws can be detected in Figs. 11c and d at 59.3 and 78.9 KHz respectively.

Test Piece 11

This sample demonstrated that a cross ply structure will enhance the detectability and identification of disbonds in a composite material. The cross ply structure provides nearly two dimensional isotropy to the sample thus making symmetrical plate modes more likely. Figure 12a, at 63.1 KHz, shows the large flaw in a two-one mode which clearly delineates the area of the unbonded area. Figure 12b, at 101.3 KHz, shows all three flaws with the shape of the large flaw well outlined. The flaws are probably also shown at several lower frequencies, but the symmetry of the modes makes positive flaw identification difficult at these frequencies.

Test Piece 12

In order to more fully evaluate the effectiveness of the HNDT method for locating flaws within the prepreg plies, a second sample, consisting of 10 plies of boron prepreg on a 10 x 15 cm aluminum substrate, was fabricated. Stainless steel bag flaws were incorporated in the 1st, 3rd, 6th, and 9th plies. The flaws near the top and bottom of the test piece, in the 1st and 6th plies as located in Fig. 13a, were identified by exciting transducers bonded to the substrate at the top and bottom respectively. No indication of the existence of the two flaws in the 3rd and 9th plies, at the intersection of the horizontal and vertical axis of the test piece, was achieved with these transducers. The transducer locations can be seen in Fig. 13b; there are two small flexural transducers at the bottom and one at the top, a larger (2.5 x 1.25 cm) flexural transducer was located at the left side on the horizontal axis as viewed from the substrate side. The cylindrical transducer with the exponential coupler in contact with the center of the test piece, which was developed for non-bonded excitation, is discussed below. Only when the large flexural transducer was driven at a high amplitude and frequency was the flaw in the third ply identifiable. It is concluded that sufficient force to overcome the pressure differential across the flaw could be obtained only at high frequencies; Fig. 13c shows the flawed area moderately well defined at 156 KHz, while Fig. 13d shows only the edge of the flaw between the transducer and the flaw at 206 KHz.

Previous tests had shown that the range of frequencies over which a flaw could just be detected was nearly one octave. (For example, a flaw whose smallest dimension was on the order of 0.625 cm was detectable over a frequency range from 50 KHz to 100 KHz.) To the extent that this is correct for all samples, it should be possible to excite the smallest flaw at the greatest possible depth at its fundamental resonance and all larger flaws should have the same mode or a higher mode at that frequency. To test this possibility and also to test the use of non-bonded transducers, an exponential horn was fabricated to couple a transducer to Test Piece No. 12. The fundamental resonant frequency of the flaw in the third ply was estimated to be 50 KHz and the flaw in the ninth ply to be 70 KHz. The peak-to-peak amplitude required to overcome the effects of ambient pressure was calculated to be 1.2 and 5 microns for the third and ninth ply flaws respectively.

With the horn coupler placed on the substrate behind the two flaws (Fig. 13b), and driven at 52 KHz, there was a five fringe peak-to-peak displacement in the area of the flaw in the third ply and the fringes were quite symmetrical in shape as shown in Fig. 14a. When the amplitude was increased to produce ten fringes on a peak-to-peak displacement of 3 microns, the fringes began to displace along the horizontal axis which tends to show the start of independent motion of the flaw in the ninth ply; this is illustrated in Fig. 14b. The drive frequency was then changed to eliminate the test piece plate modes in order to demonstrate the potential advantage in flaw definition which could be obtained by using traveling waves for this type of HNDT; this is illustrated in Fig. 14c.

NASA Flaw Sample

Further evaluation of the non-bonded transducer technique was performed with a NASA supplied sample. It consisted of boron epoxy prepreg bonded to a titanium substrate with flaw locations and sizes, viewed from the prepreg side, as shown in Fig. 15a. The flaws are 4 mil thick resistance welded stainless steel bags. From top to bottom the horizontal rows of flaws are mounted in successively deeper plies. The plate was driven, with the transducer horn coupler, at 52 KHz near the center of the plate and the delineation of the flaws from the holographic reconstruction is clearly shown in Fig. 15b. The flaw in the lower left-hand corner is not clearly identified, but its calculated fundamental resonant frequency is 70 KHz; it is probable that if such an excitation frequency had been used, all the flaws would have been identified.

THERMAL STRESSING AND REAL-TIME HOLOGRAPHY

In addition to the ultrasonic work, and under Corporate funding, another form of low-level stressing (thermal) was studied as a potential technique for detecting disbonds in boron-epoxy prepreg bonded to an aluminum substrate. The technique involves establishing a mild thermal gradient ($\Delta T = 5^{o}C$) in a test piece of composite material and observing, in real-time, the resulting holographic fringe pattern. The real-time holographic process is used as it permits changes in the fringe pattern to be observed as a function of time and as such, facilitates detection of any surface variations.

The thermal gradient is established by rapidly heating the prepreg surface with a tungsten iodide lamp, and air cooling the aluminum surface (holographic observation is on the prepreg side). In this manner, any interruption in the rate of heat conduction through the sample, caused by a flaw or void in the bond, will result in a change in the thermal expansion or contraction of the surface in the flawed regions. These minute surface variations can then be detected as irregularities in the holographic interferometric fringe pattern.

Test Pieces 1, 2, 3 and 4 were used to evaluate this technique. In the experimental setup, the sample was clamped between an air cooled copper heat sink and a piece of plexiglass. The plexiglass served two purposes: 1) it provided the sample with even contact to the heat sink, thus eliminating improper contact as a possible cource of interferometric fringe irregularities; and 2) it reduced thermal bowing due to differences in the expansion coefficients of the boron-epoxy and aluminum, which would create a fringe pattern of its own, tending to mask the smaller surface changes caused by the flaw. It should be noted that the use of a heat sink and the plexiglass surface clamp would not be necessary in a large sample where the more rapid flow of heat in the sample would tend to negate the fringe effects mentioned above.

A typical experimental result on Test Piece 1 is presented in Fig. 16, which shows a photographic sequence made on the real-time holographic set up. The photographs were recorded, after mild thermal stressing, immediately after and at 5 minute intervals as the sample was cooling. As can be seen, the test piece has a fairly uniform fringe pattern over the sample surface except in the region of the programmed flaw. In this area the fringe density is much higher and the shape of the fringes highly irregular. This indicates that there is a greater surface expansion in this region where the heat conduction is less rapid, as would be expected for an air gap type flaw. In addition to the still photographs, a 16 mm black and white movie was made of the test piece while it was being thermally stressed in the holographic setup. Analysis of the film showed that the debonded region could be observed much more readily the first few seconds after thermal stressing because of the dynamic character of the fringes. From these results it

would appear that the still photographs, as well as latter portions of the movie, do not depict the debonded region as dramatically as does dynamic fringe observation immediately after thermal stressing.

The testing of Samples 2, 3 and 4 by thermally stressing them between the air cooled copper heat sink and the piece of plexiglass showed negative results. No debonds were evident by either visual real-time observation or in the 16 mm movies made during the tests. It was concluded that the negative results were caused by lack of a sufficient thermal gradient across the test pieces. This problem did not arise when Test Piece No. 1 was tested in this manner since it had an air gap as a bond flaw, and the heat transfer across the defect was drastically different than in the surrounding material. However, in Test Pieces 2, 3 and 4 the bond flaws were vacuum voids, produced by the insertion of welded stainless steel bags (3, 4) or a Mylar disc (2) into the test piece, rather than air gaps. For such a flaw, the heat transfer in the debonded region is not much different than in the surrounding material and thus, to detect the flaws, a stronger thermal gradient is required. However, it was impossible to apply a stronger thermal gradient to the sample while it was clamped between the copper heat sink and the plexiglass for two reasons: 1) this arrangement prevented the application of heat directly to the sample; and 2) thermal bowing, though restricted somewhat by the clamping arrangement could not be entirely prevented at the temperature differences required to establish a sufficient thermal gradient.

In order to apply the required gradient, and still eliminate the thermal bowing, a new clamping and thermal stressing technique was devised. The clamping technique consisted of rigidly securing one end of the test piece and then pre-stressing the piece, by applying a force to the opposite end, before making the real-time hologram. The force is applied in order to bow the test piece in the same direction as it would bow upon heating or cooling. Thus thermal bowing of the test piece when heat is applied or removed will be minimized until the pre-applied stress is overcome. The thermal gradient was applied by cooling the aluminum side of the test piece with liquid nitrogen cooled air and heating the prepreg side with a tungsten iodide lamp. In this manner, a temperature gradient of approximately 10° to 15°C was produced.

Test Piece No. 4 was used to evaluate this technique. Visual observation of the test piece under real-time holographic conditions showed that the debond regions could be observed, but only after the lamp had been removed and the sample was cooling. In an equilibrium state the flaws were not observed.

This technique was also applied to the NASA tensile test specimen; a 30 x 5 cm boron-epoxy prepreg and aluminum panel. The panel had an Elox slot in the aluminum substrate and had been subjected to cyclic loading causing a crack to develop and propagate outward approximately 1.25 cm from either end of the slot. Because of the overall size of the sample no special considerations had to be given to prevent thermal bowing or increase the heat flow when establishing the

thermal gradient. The sample was loosely clamped at both ends and a gradient established by flowing acetone onto the aluminum surface (the evaporation of the acetone causes a mild cooling to take place). In this manner, an elliptical flaw, approximately 2.0 x 1.0 cm and centered about the Elox slot with the major axis parallel to the crack, was observed.

In conclusion, this technique suggests one potentially attractive method for the eventual establishment of a practical holographic inspection system. The main advantage of the method is the extreme ease of application. However, a disadvantage is that thermal stressing does not delineate the flawed region as well as acoustic stressing and it is difficult to determine the depth of the flawed area. Additionally, the technique requires the use of real-time holography and observation of a dynamic fringe pattern. The direct observation of this type of pattern over a period of time, as would be required in an inspection procedure, becomes extremely fatiguing.

THERMAL MAPPING WITH AN IR SCANNING CAMERA

In addition to the ultrasonic excitation and thermal gradient investigations, an infrared (IR) scanning camera was used to examine Test Piece Nos. 1, 4, 5, 7 and 8 and the NASA Tensile Test Specimen. The technique is similar to the preceding thermal holographic work in that a temperature gradient is established in the test piece. However, the IR camera records the surface temperature of the test piece, rather than the surface displacement, and requires a larger thermal gradient (approximately 50°C) to work effectively. The thermal gradient is applied by heating the aluminum surface of the composite sample with a hot plate, or tungsten iodide lamp, and cooling the prepreg surface with a room temperature air blower.

Test Piece Nos. 1, 4, 5, 7 and 8 all showed indication of a lower surface temperature (darker area) at the flawed regions when tested in this manner. All, however, were not marked indications of the flaws but were barely discernable from the background noise. Polaroid photographs were taken of the scanning camera's display oscilloscope and representative results for Test Piece Nos. 4 and 5 are presented in Fig. 17 and Test Piece Nos. 7 and 8 are presented in Fig. 18. As can be seen in Fig. 17 the flaws are barely visible; however, it can be noticed that, in general, the stainless steel bag flaws are more visible than the Mylar flaws. This is attributed to the differences in thermal conduction between the two types of materials. In Fig. 18 only the larger of the three flaws in Test Piece 7 is visible. The two smaller flaws could be detected only with a great degree of difficulty using various heating and cooling configurations; however, the three flaws were never detected simultaneously. The primary reason for this was that the same temperature could not be established over the entire test piece. In Test Piece 8 both flaws were detectable simultaneously. As seen in Fig. 18, the flawed area at the top is somewhat darker (lower surface temperature) than the flawed area at the bottom. This suggests that there is a slight difference in thermal conductivity between the UARL manufactured stainless steel bag (top) and the NASA manufactured bag (bottom). A possible cause for this difference could be the amounts of residual gas left in the stainless steel bags after evacuation.

The detection of all of the above flaws is somewhat easier by direct observation of the display scope since the eye has a greater intensity latitude than photographic film; but in all of these cases the flaw definition is poor. In addition to the recording problem, not all of the defects are visible at the same time, as in Test Piece 7. Different heating and cooling configurations were required in order to positively identify any one defect well.

Finally, the flaw in the NASA Tensile Test Specimen was not detectable using the IR scanning camera technique.

CONCLUDING REMARKS

The reliability of identifying unbonded areas in thin composites is dependent upon the ability to excite a mode which is unique to the plate area above the disbond. The resonant frequency of any such mode (one which can be generated in a plate above an unbonded area) is directly proportional to the plate thickness, inversely proportional to the area of unbond, and a function of the dimension along the fiber axis (high modulus axis) as described below. The minimum frequency at which it might be possible to detect all significant unbonded areas must be determined by the resonant frequency of the smallest significant area at the greatest possible depth.

In boron and carbon epoxy matrixes, the mechanical Q's* have been found to be quite low. Consequently, if the smallest area of interest is driven with sufficient amplitude to produce a few interference fringes, all larger areas will also be identifiable in that mode or a higher order mode. If the boron prepreg is considerably thicker than the substrate, some unbonded areas may be more easily detected on the substrate side; in such a case, two different excitation frequencies may be required. In materials with high mechanical Q's, such as borsic aluminum matrixes, it may be necessary to limit the amplitude of drive to prevent loss of resolution in the hologram. Consequently, higher modes may not become detectable before the lower order modes are lost; in such a case additional excitation frequencies may be necessary to detect all unbonded areas of interest. In structures with uniaxial fibers, the minimum frequency is determined by the shortest possible unbonded length along the fiber axis since that modulus is much greater than along the axis perpendicular to the fiber. Consequently, the minimum frequency can be calculated with sufficient accuracy either by considering the length along the fiber as a bar clamped at both ends or a clamped circular plate with that diameter.

If the unbonded area is a good vacuum, or if the "unbonded" area is really a very weak bond, sufficiently high excitation amplitudes must be used to "release" the unbonded area. For example, the 0.625 x 1.875 cm stainless steel bag located in the third ply (from the substrate) of a ten ply prepreg, with the 1.875 cm dimensions along the fiber axis, would have a resonant frequency of 50 KHz, and at that frequency a peak-to-peak amplitude of 1.2 microns would be required to separate the bag walls. It has been shown that detection is more certain if the composite piece is excited in such a way that it is not at resonance. In this case, the vibrations above the unbonded areas will not be obscured. This may be accomplished by either damping the edges of the piece or using a non-resonant excitation frequency. However, in this case, the drive must be doubled.

* The mechanical Q is defined as the frequency ratio $f_p/\Delta f$, where f_p is the frequency at the peak vibrational amplitude, and Δf is the difference between the frequencies for which the vibrational amplitude is 0.707 of the peak amplitude on either side of resonance.

A practical way of coupling the output of a very large transducer, one that could not be attached to a piece for flexurally generated vibrations, is to use the exponential horn device described earlier. However, the amplitude of vibration produced by the exponential coupler cannot be greater than the transducer amplitude for an area greater than the transducer cross sectional area. Nevertheless, the test area can be significantly increased in this way, and the test time, in a practical situation, decreased considerably.

Much of the flaw identification obtained with bonded flexure transducers was not as certain as would be desired. The use of vacuum unbonds required high amplitude drive with resulting thermal distortions. In some cases, when the excitation was continued until thermal equilibrium was established, the bond strength of the transducer was reduced. This was, however, a useful way of obtaining frequency information without fabricating a large number of transducers. On the other hand, the data obtained with the exponential horn coupler was far more definitive; no thermal problems were introduced, the bonding process was eliminated, greater amplitude drive was possible, and the results demonstrated only begin to approach the potential quality of a system designed on the basis of this investigation.

RECOMMENDATIONS

The establishment of a practical holographic inspection system will require an investigation of various simple methods for introducing high frequency acoustic energy into a test specimen and the applicability of these methods to large composite structures. A practical method for introducing acoustic energy would be one in which no adhesive bonds are made to the test specimen and one in which complete mobility is afforded. The amount of energy which can be introduced into a test specimen is another practical consideration since the inspection of large structures will necessitate the use of traveling acoustic waves as opposed to standing acoustic waves, which were utilized for the major portion of the present work. The preliminary studies with a nonbonded exponential horn, during the course of the present contract, gave evidence of being one potential solution to the problem.

Two further areas of interest are: a study of the effectiveness of the technique as applied to different materials (metal matrix composites and polyimide structures are two potential material candidates which should be given consideration); and, an evaluation of the applicability of the method to large composite structures.

In addition to developing a practical inspection technique, evaluation as to the effect disbonds have on the overall strength of a composite material should also be made. Without such an evaluation, a decision of acceptance or rejection of a particular composite structure cannot be made effectively since the existence, and detection, of a bond flaw would not, a priori, impair the overall structural integrity. To just discard all parts found with flaws would be impractical since the material and labor costs in fabricating a large composite structure are extremely high. Therefore, a relationship between the flaw size and shape to overall structural strength must be established. One potential approach to this problem would be an investigation of single lap shear specimens with varying areas of disbond. Holographic nondestructive testing of such samples should be combined with destructive testing studies to establish the proper correlation factors.

Finally, consideration should be given to adapting the technique for determining bond quality, as opposed to just characterizing the size, shape and location of total disbonds. At high excitation frequencies (above 100 KHz), the absorption and complex modulus of adhesive materials cause phase and propagation changes in the deformation of composite surfaces which potentially can be used to describe the properties of the forming structure of the composite. The physical properties of most adhesives are significantly different than metallic structural material. The modulii span a large range and are complex in nature; that is, upon acoustic excitation the change in pressure lags the change in

deformation due to viscosity and heat conduction losses. Less than maximum adhesion will cause an apparent decrease in the adhesive modulus and, for the same amplitude of vibration, the acoustic attenuation will be greater. Decreases in cohesion also decrease the elastic modulus and increase the attenuation. Preliminary study of increases in driving amplitude or duration of excitation have made these effects evident. The phase lag, due to the complex modulus of the adhesive, makes possible the simultaneous occurence of shear and longitudinal stresses; further, the frequency at which this occurs is a measure of the similarity between a test sample and an optimum (well bonded) sample. In summary, the evidence to date clearly indicates that further study of ultrasonic plate vibrations, together with interferometric holography, in composite structures offers considerable promise in the area of bond strength measurements.

The ground work for investigations in all of the above areas has been laid both previous to, and during the just completed contract period; consequently, the continuing studies can be initiated immediately. Indeed, they represent the logical "next-steps" in a continuing program to establish a practical holographic inspection system for composites. Therefore, it is recommended that one or more of the following studies be pursued at this time.

1 - Further study and development of an effectual acoustic excitation technique, such as the horn drive system, to facilitate implementation of the holographic nondestructive testing process.

2 - Application of the technique to other composite materials.

3 - Demonstration of the technique as applied to large composite structures.

4 - An investigation to determine the relationship between composite shear strength and disbond characteristics.

5 - A feasibility study to evaluate the applicability of holographic nondestructive testing methods for determining bond quality.

APPENDIX I

DESCRIPTIONS OF TEST SAMPLES FABRICATED AT UNITED AIRCRAFT RESEARCH LABORATORIES

Test Piece 1. A triangle of Teflon was placed between the prepreg (4 plies of boron epoxy previously bonded) and an 0.8 mm thick aluminum substrate. The triangle had a 1.25 cm base and a 2.5 cm height and was placed with its base along one edge of the sample. After the adhesive cured, the Teflon was pulled from between the prepreg and substrate leaving a void in the bond. (Although the entire piece was not removed, probing with a small wire indicated that a large portion had been removed.)

Test Piece 2. A single elliptical flaw was programmed in the sample in the following manner: a 1.875 cm diameter circle was milled out of the substrate material (0.8 mm aluminum) to a depth of 0.1 mm and a 1.875 cm diameter, 0.125 mm thick Mylar disc was placed in the cavity; a 1.25 cm diameter portion in the center of the mylar was clamped while the outer annulus was bonded to the aluminum. Some adhesive did flow under the clamped area and the final area of debond was an ellipse with axes of approximately 0.5 x 0.8 cm. No separation between the mylar and the aluminum could be detected while viewing the unbonded area with a microscope during flexing of the aluminum. After inspection, the defect area was abraded until it was nearly even with the remainder of the sample, and the 4-ply boron prepreg layer was then bonded to the defect side of the substrate.

Test Piece 3. Three programmed rectangular flaws (electron beam welded stainless steel bags) were incorporated in the sample by cutting out corresponding areas in the boron prepreg ply adjacent to the 0.8 mm thick aluminum substrate. Two of the flaws were approximately 1 x 1 cm and the third was approximately 1 x 0.5 cm. The sample was prepared by the two-step bonding process.

Test Piece 4. Similar to test piece 3 with the exception that one of the 1 x 1 cm flaws in the first ply was removed and an 0.5 x 0.3 cm stainless steel bag was incorporated in the third ply, counting from the substrate. In addition, the substrate was twice as thick (1.6 mm) and the sample was fabricated in a one-step bonding process.

Test Piece 5. Two 0.025 mm thick Mylar patches were bonded to an 0.8 mm thick aluminum substrate using the clamping procedure employed for Test Piece No. 2. The large Mylar flaw was 1.25 cm in diameter, and the small Mylar flaw was 0.625 cm in diameter. Also included in this sample was a stainless steel bag.

Test Piece 6. One programmed rectangular flaw was incorporated in the sample in the following manner: the flaw was created by cutting a 1.25 x 1.25 cm piece of material out of a sheet adhesive (B. F. Goodrich Plastilock 729) used to bond the prepreg material (4 plies of previously bonded boron epoxy) to a 1.5 mm thick glass substrate, which had been previously sprayed with a release agent at the location of the flaw.

Test Piece 7. Three programmed rectangular flaws (0.5 x 0.5 cm, 1 x 0.5 cm and 1 x 1 cm electron beam welded stainless steel bags) were incorporated in the sample by cutting out corresponding areas in the ply adjacent to the substrate and bonding five plies of boron epoxy prepreg to an 0.75 mm titanium substrate in a one-step process.

Test Piece 8. Two programmed rectangular flaws (0.8 x 1.25 cm stainless steel bags) were incorporated in a sample consisting of five plies of boron epoxy prepreg bonded to an 0.8 mm thick aluminum substrate in a one-step process. One of the stainless steel bags was fabricated by electron beam welding and the other, supplied by NASA, by resistance welding. Both bags had been evacuated: one by virtue of the electron beam welding process; and the other by evacuation after an initial resistance welding step.

Test Piece 9. A single programmed rectangular flaw (approximately 2.5 x 2.5 cm electron beam welded stainless steel bag) was incorporated in the first ply of a sample consisting of 10 plies of boron epoxy prepreg bonded to an 0.8 mm thick aluminum substrate in a one-step process.

Test Piece 10. Three programmed rectangular flaws (0.5 x 0.625 cm, 0.5 x 1 cm, and 1 x 1 cm electron beam welded stainless steel bags) were incorporated in the sample by cutting out corresponding areas in the ply adjacent to the substrate and bonding five plies of carbon epoxy prepreg to an 0.75 mm thick titanium substrate in a one-step process. The carbon prepreg was manufactured by impregnating Thornel T-50s graphite yarn (modulus = 58×10^6 psi) with 2256 Bakelite resin and 0820 Bakelite hardener.

Test Piece 11. Three programmed rectangular flaws (0.5 x 0.625 cm, 1.25 x 1.25 cm, and 0.5 x 1 cm electron beam welded stainless steel bags) were incorporated in a sample consisting of five cross plies of boron epoxy prepreg bonded to an 0.8 mm thick aluminum substrate in a one-step process. The successive plies from the substrate to the surface were oriented at 0°, 45°, 90°, 135°, and 0°. As in Test Piece No. 10, the flaws were incorporated in the ply adjacent to the substrate by cutting out areas corresponding to the stainless steel bag dimensions.

Test Piece 12. Four programmed rectangular flaws were incorporated in a sample consisting of 10 plies of boron epoxy prepreg bonded to a 10 x 15 cm aluminum substrate of 0.8 mm thickness. The sample was fabricated by cutting out an area for each of the four flaws in various plies and inserting an electron beam welded stainless steel bag of equal area and bonding all 10 plies to the substrate in a one-step process. The flaws were positioned in the sample in the following manner: a 1.25 x 1.875 cm flaw in the first ply; an 0.625 x 1.875 cm flaw in the third ply; an 0.625 x 1.875 cm flaw in the sixth ply; and an 0.625 x 1.875 cm flaw in the ninth ply. The flaws in the first and sixth plies were near the ends of the test piece. The flaw in the third ply was at the center of the test piece with the long dimension (1.875 cm) perpendicular to the fibers, and the flaw in the ninth ply was located symmetrically over the flaw in the third ply, but with its long dimension parallel to the fibers.

REFERENCES

1. Erf, R. K., H. G. Aas, and J. P. Waters, Jorn. of the Acous. Soc. of Am., Vol. 47, 1970, p. 968.

2. Morse, Philip M., Vibration and Sound, 2nd Edition, McGraw-Hill Book Co., Inc., New York, 1948, p. 210.

3. Skudrzyk, Eugene, Simple and Complex Vibratory Systems, Penn. State University Press, University Park, 1968, p. 249.

4. Mason, Warren P., Physical Acoustics and the Properties of Solids, D. Van Nostrand, Inc., New York, 1958, p. 158.

TABLE 1

COMPOSITE SAMPLE SPECIFICATIONS

Sample	Size (cm)	Prepreg Material	No. of Plies	Substrate Thickness (mm)	Bonding Steps	Flaws	Flaw Size (cm)	Location	Ultrasonic	Thermal	IR Scanning	Remarks
1	5x10	B	4	Al,0.8	2	1-Teflon	1.25x2.5	S	X	X	X	Defective adhesive; size and shape of flaw identifiable by all three techniques; holography superior. (Figs. 3 and 16)
2	5x10	B	4	Al,0.8	2	1-Mylar	0.5x0.8	S	X	X		Flaw identifiable by ultrasonic method.(Fig.3)
3	5x10	B	4	Al,0.8	2	2-S.S.B.* 1-S.S.B.	1.0x1.0 1.0x0.5	1st 1st	X	X		Because of acoustically lossy adhesive, clamping required to increase ultrasonic amplitude and identify flaw; no thermal result. (Fig. 4)
4	5x10	B	4	Al,1.6	1	1-S.S.B. 1-S.S.B. 1-S.S.B.	1.0x1.0 1.0x0.5 0.5x0.3	1st 1st 3rd	X	X	X	Flaws in 1st ply identifiable, but insufficient vibrational amplitude to identify flaw in 3rd ply; holography superior. (Figs. 5 and 17)
5	5x10	B	4	Al,0.8	2	1-Mylar 1-Mylar 1-S.S.B.	1.25 dia. 0.625 dia. 1.6x0.625	S S S	X		X	Mylar flaws identifiable, stainless steel bag was not ultrasonically. (Figs. 6 & 17)
6	5x10	B	4	Glass, 1.5	2	1-No Adhesive	1.25-1.25	S				For studying effects of sheet adhesive and release agent. (Fig. 7)
7	5x10	B	5	Ti,0.75	1	1-S.S.B. 1-S.S.B. 1-S.S.B.	1.0x1.0 1.0x0.5 0.5x0.5	1st 1st 1st	X		X	Evaluate effect of titanium substrate; all flaws identifiable, both size and shape; holography superior. (Figs. 8 and 18)
8	5x10	B	5	Al,0.8	1	2-S.S.B.	0.8x1.25	1st	X		X	Evaluate difference between resistance welding and electron beam welding of S.S. bags; both flaws identifiable; good thermogram. (Figs. 9 and 18)
9	5x10	B	10	Al,0.8	1	1-S.S.B.	2.5x2.5	1st	X			Flaw identifiable; used to evaluate technique on thick composites. (Fig. 10).
10	5x10	C	5	Ti,0.75	1	1-S.S.B. 1-S.S.B. 1-S.S.B.	0.5x0.625 0.5x1.0 1.0x1.0	1st 1st 1st	X			Evaluate technique on graphite composites; all flaws identifiable. (Fig. 11)
11	5x10	B	5	Al,0.8	1	1-S.S.B. 1-S.S.B. 1-S.S.B.	0.5x0.625 1.25x1.25 1.0x0.5	1st 1st 1st	X			Evaluate effects of crossed plies; all flaws identifiable; size and shape of large flaw clearly defined. (Fig. 12)
12	10x15	B	10	Al,0.8	1	1-S.S.B. 1-S.S.B. 1-S.S.B. 1-S.S.B.	0.625x1.875 0.625x1.875 0.625x1.875 1.25x1.875	9th 6th 3rd 1st	X			Further study of method for finding flaws within the plies; exponential transducer drive employed; all flaws identified except one in 9th ply. (Figs. 13 and 14)
NASA	15x15	B	5	Ti	1	4-S.S.B. 4-S.S.B. 4-S.S.B.	2.5x6.25 1.25x1.25 1.25x0.625	1,2,3,4 1,2,3,4 1,2,3,4	X			11 of the 12 flaws identified with exponential transducer drive. (Fig. 15)
NASA	30x5	B		Al		1-Crack	2.5	S		X	X	Tensile test specimen - identified with thermal stressing.

* S.S.B. denotes Stainless Steel Bag

FIG. 1

EXPONENTIAL HORN TRANSDUCER

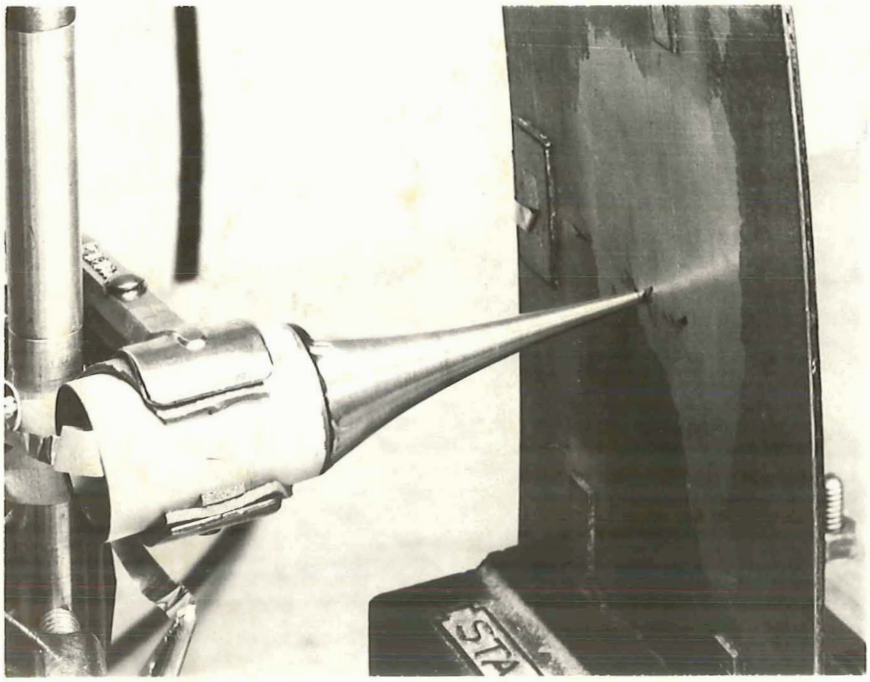

COMPOSITE MATERIALS

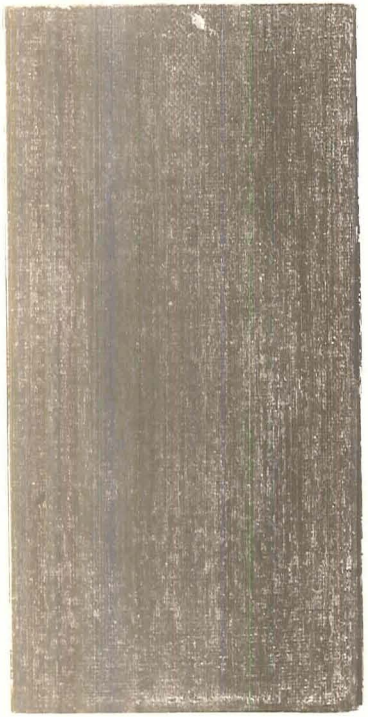

(a) BORON PREPREG

(b) ALUMINUM SUBSTRATE

(c) CARBON PREPREG

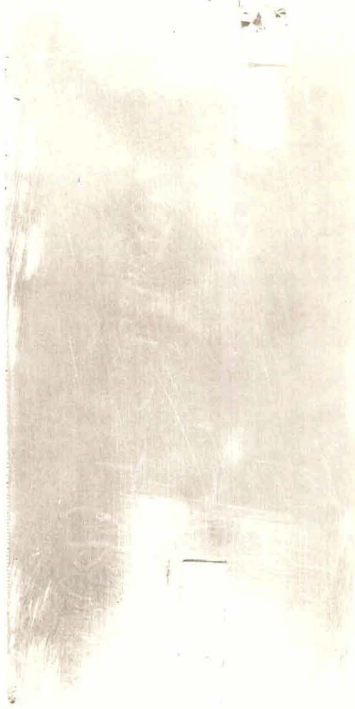

(d) TITANIUM SUBSTRATE

FIG. 2

COMPOSITE BOND INSPECTION

HOLOGRAPHIC RECONSTRUCTIONS

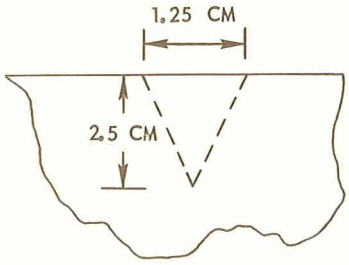

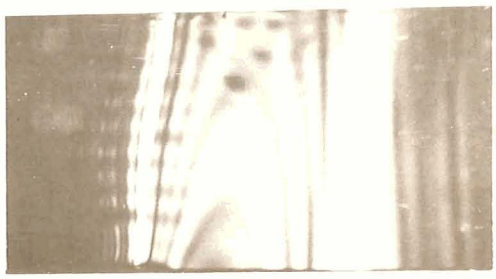

(a) TEFLON TRIANGULAR FLAW – BORON EPOXY PREPREG AND ALUMINUM
ULTRASONIC EXCITATION FREQUENCY – 90 KHz

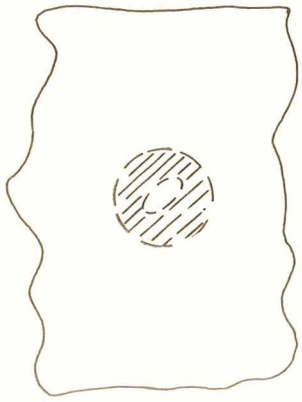

(b) CAVITY & MYLAR DISC FLAW – BORON EPOXY PREPREG AND ALUMINUM
ULTRASONIC EXCITATION FREQUENCY – 111 KHz

COMPOSITE BOND INSPECTION

EFFECTS OF CLAMPING ON FLAW DETECTION

TEST PIECE 3 – BORON PREPREG AND ALUMINUM

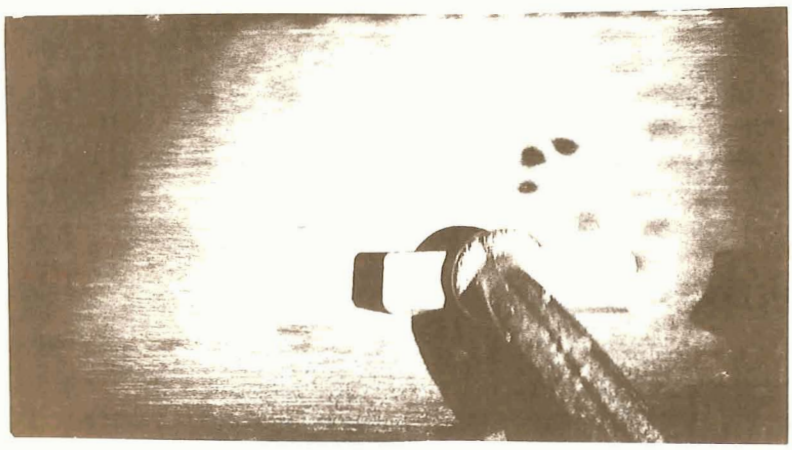

(a) GRAZING INCIDENCE – 126.2 KHz

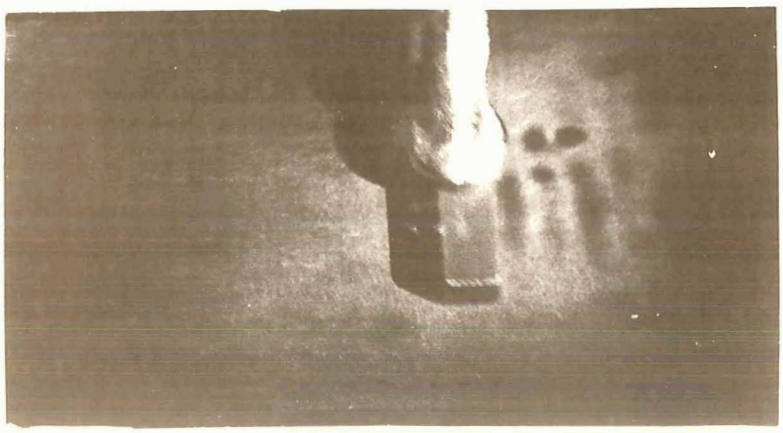

(b) PERPENDICULAR INCIDENCE – 126.0 KHz

COMPOSITE BOND INSPECTION

HOLOGRAPHIC RECONSTRUCTION

TEST PIECE 4 —STAINLESS STEEL BAG FLAWS

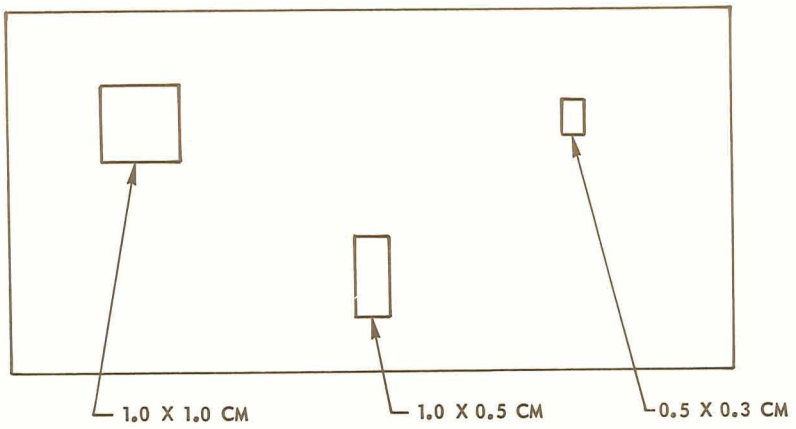

(a) FLAW LOCATION

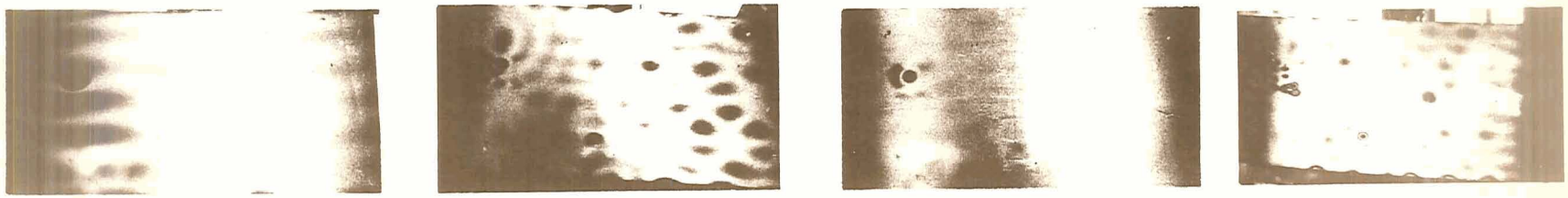

45.4 KHz | 101.8 KHz | 104.5 KHz | 121.4 KHz

(b) FLAW IDENTIFICATION

FIG. 5

COMPOSITE BOND INSPECTION

TEST PIECE 5

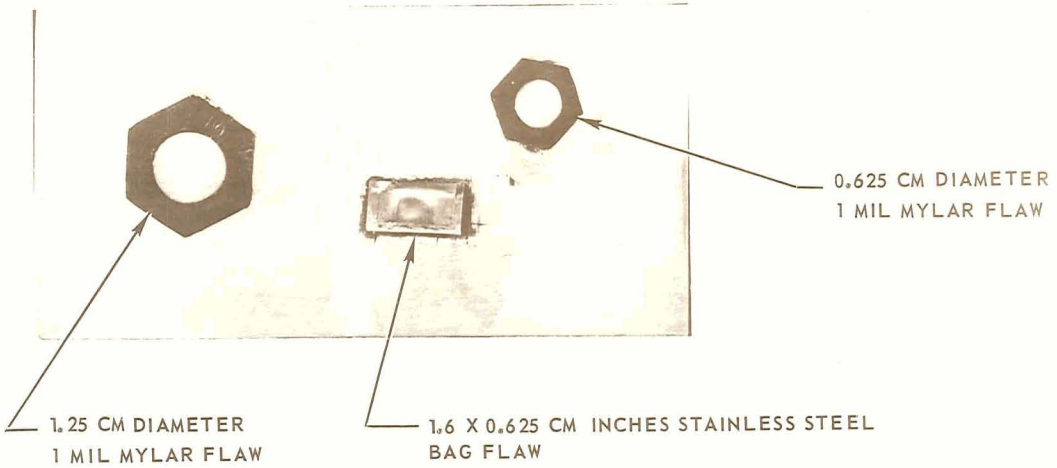

(a.) FLAW LOCATION

119.4 KHz | 71.8 KHz | 43.8 KHz | 120 KHz MIRROR IMAGE

(b.) FLAW IDENTIFICATION

FIG. 6

COMPOSITE BOND INSPECTION

RELEASE AGENT EFFECTS ON SHEET ADHESIVE FLAWS

TEST PIECE 6 – BORON PREPREG AND GLASS

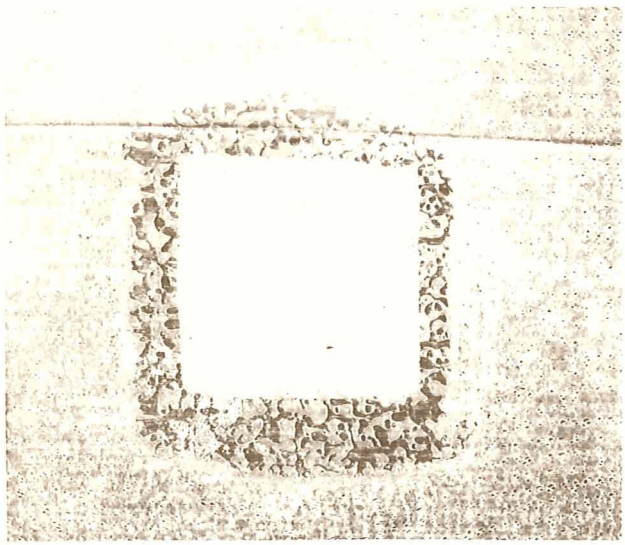

(a)

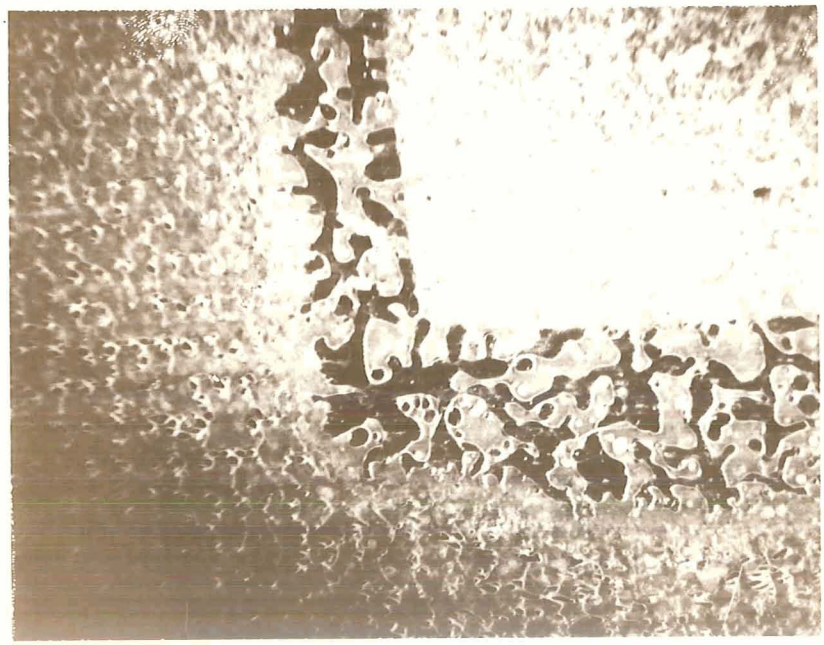

(b)

FIG. 8

COMPOSITE BOND INSPECTION

STAINLESS STEEL BAG FLAWS

TEST PIECE 7 – BORON PREPREG AND TITANIUM

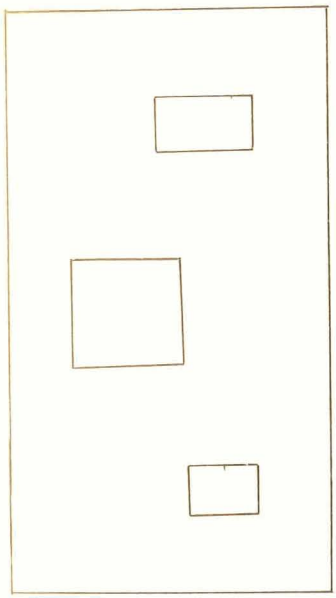

(a) SCHEMATIC

(b) 72.5 KHz

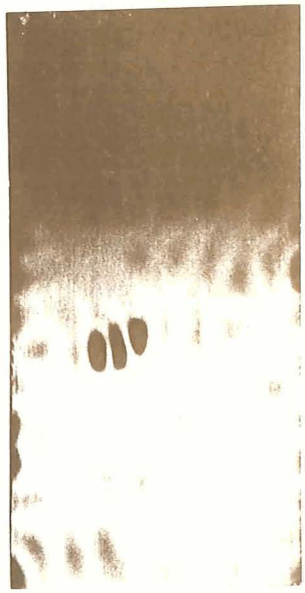

(c) 83.5 KHz

(d) 107.0 KHz

(e) 115.4 KHz

(f) 142.0 KHz

COMPOSITE BOND INSPECTION

STAINLESS STEEL BAG FLAWS

TEST PIECE 8 – BORON PREPREG AND ALUMINUM

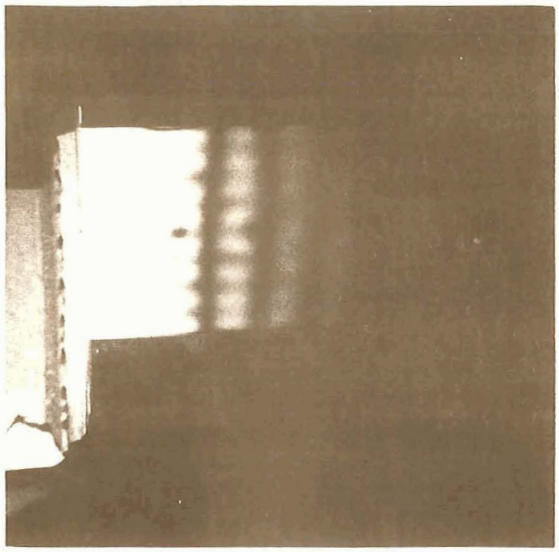

(a) 56.9 KHz UARL ELECTRON BEAM WELDED BAG

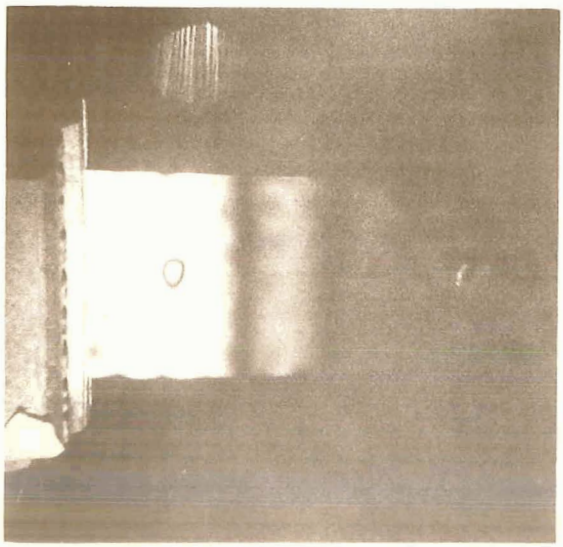

(b) 50.8 KHz NASA RESISTANCE WELDED BAG

COMPOSITE BOND INSPECTION
STAINLESS STEEL BAG FLAWS

TEST PIECE 9 – 10 PLY BORON PREPREG AND ALUMINUM

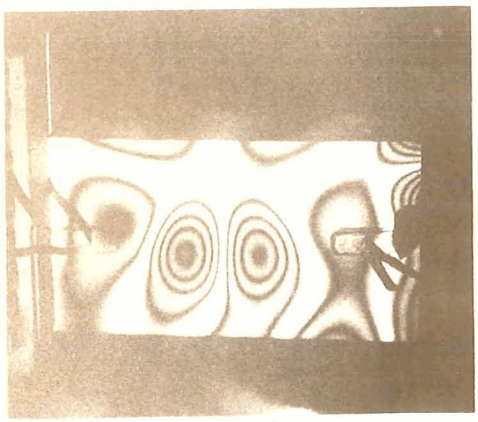

(a) 10.8 KHz SUBSTRATE SIDE

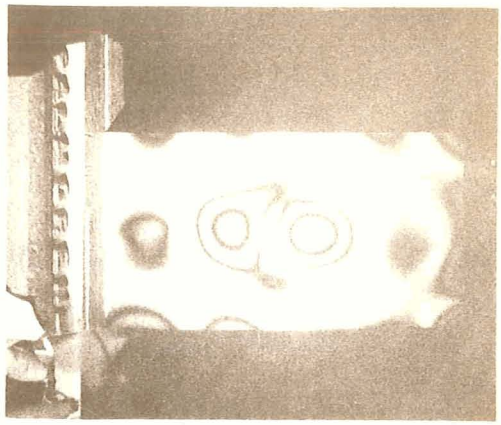

(b) 15.0 KHz PREPREG SIDE

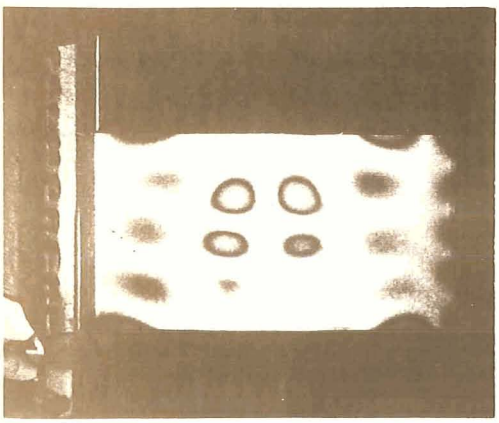

(c) 23.8 KHz PREPREG SIDE

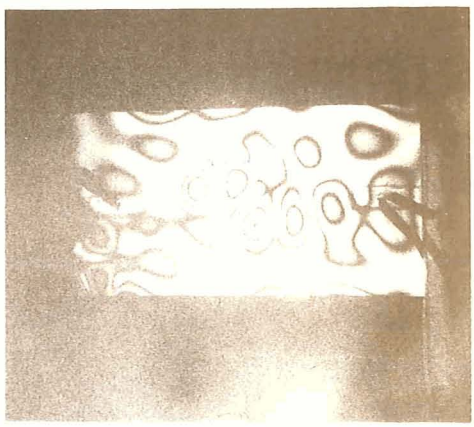

(d) 29.9 KHz SUBSTRATE SIDE

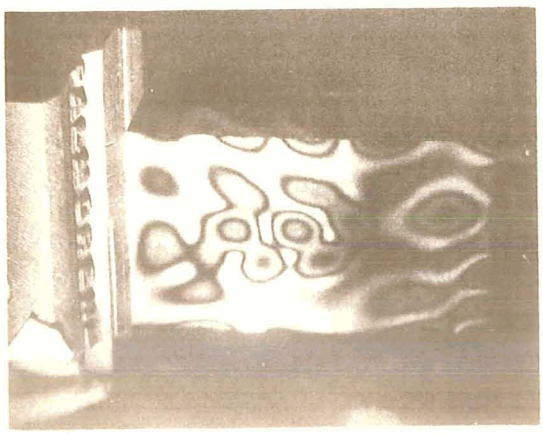

(e) 29.4 KHz PREPREG SIDE

COMPOSITE BOND INSPECTION
STAINLESS STEEL BAG FLAWS

TEST PIECE 10 – CARBON EPOXY AND TITANIUM

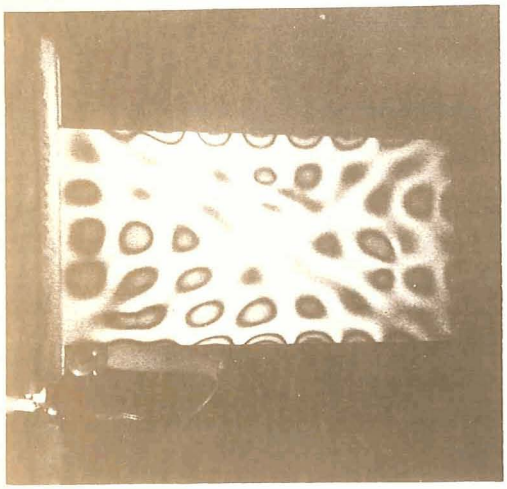

(a) 44.8 KHz

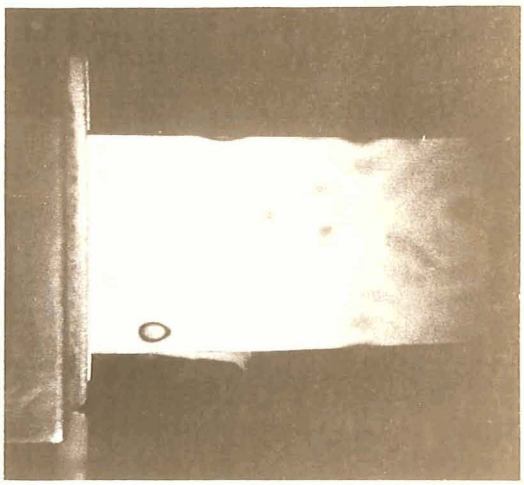

(b) 49.3 KHz

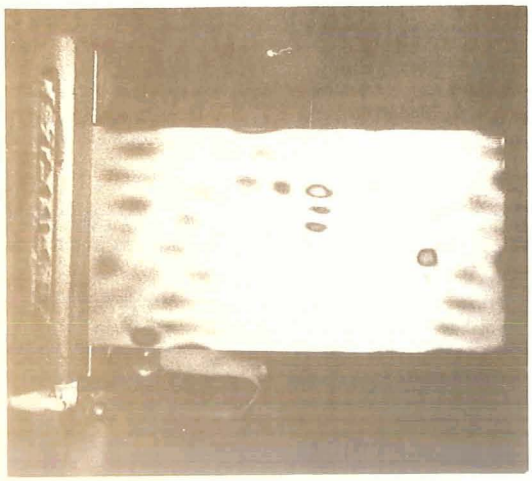

(c) 59.3 KHz

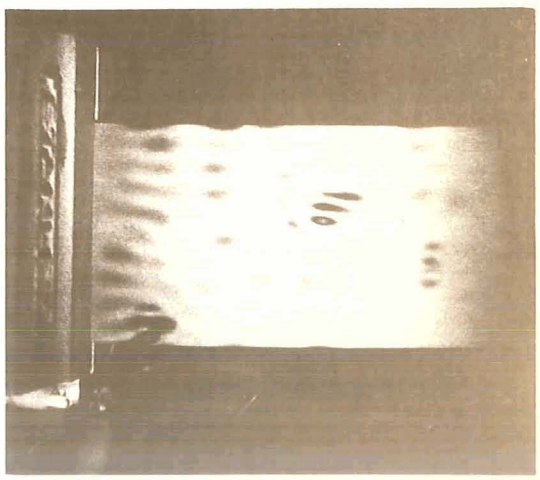

(d) 78.9 KHz

COMPOSITE BOND INSPECTION
STAINLESS STEEL BAG FLAWS

TEST PIECE 11 – CROSSED PLY BORON PREPREG AND ALUMINUM

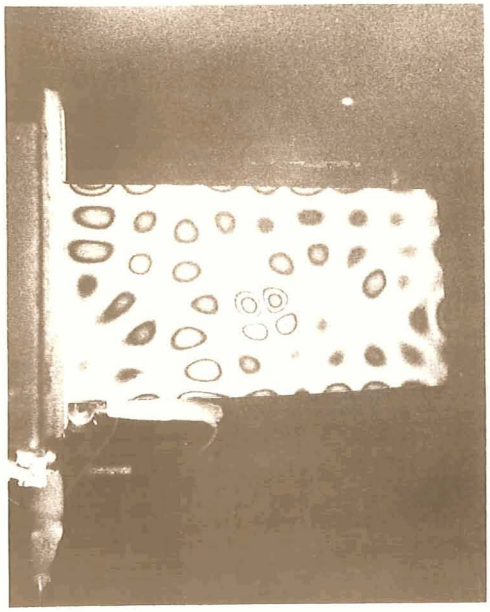

(a) 63.1 KHz

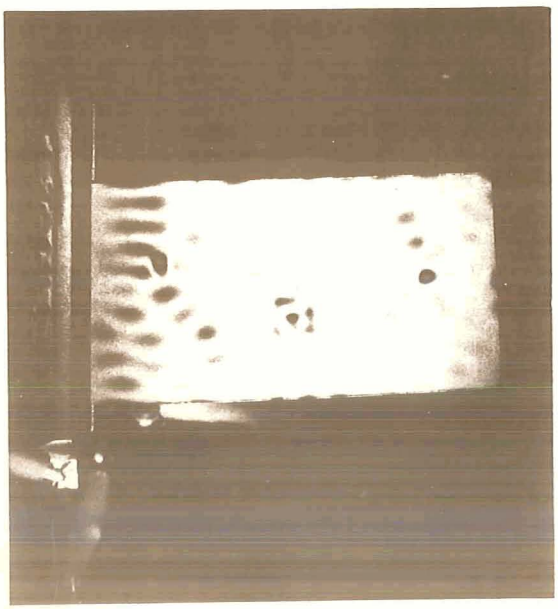

(b) 101.3 KHz

COMPOSITE BOND INSPECTION
STAINLESS STEEL BAG FLAWS
TEST PIECE 12–10 PLY BORON PREPREG AND ALUMINUM
FLEXURAL DRIVE

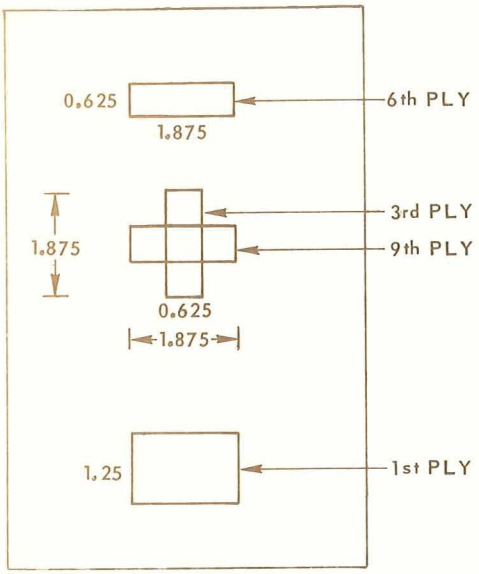

(a) FLAW LOCATION

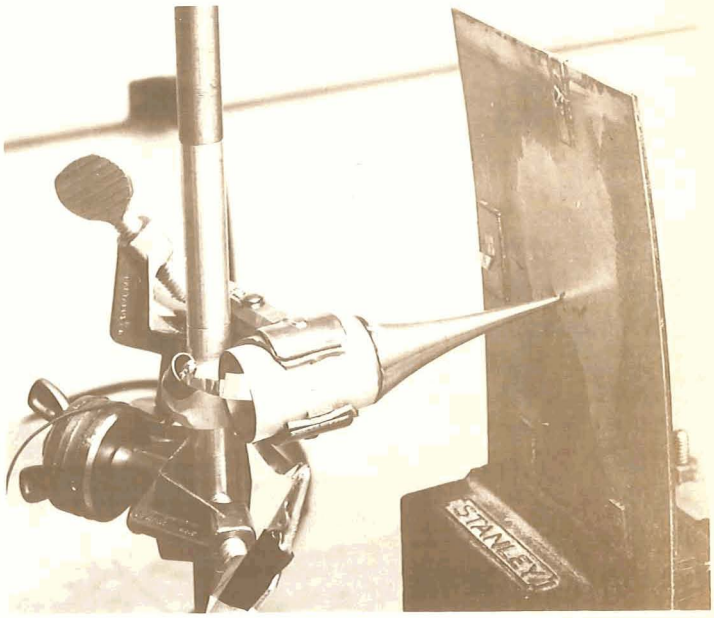

(b) TRANSDUCER LOCATION

(c) FLEXURALLY INDUCED VIBRATIONS 156 KHz

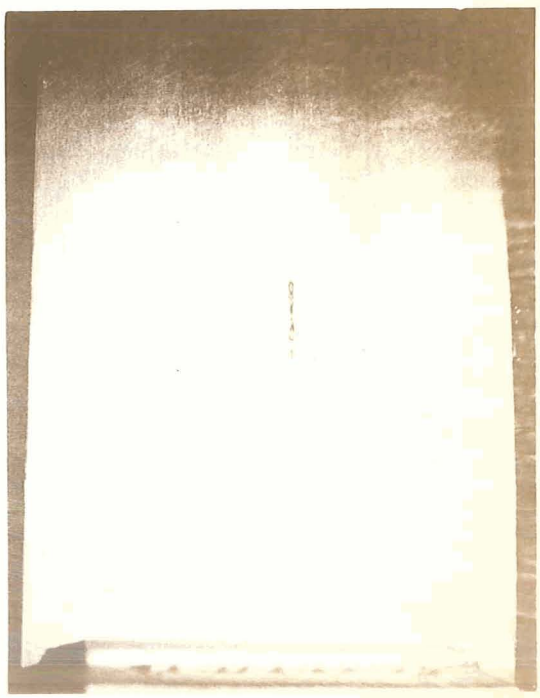

(d) FLEXURALLY INDUCED VIBRATIONS 206 KHz

COMPOSITE BOND INSPECTION

STAINLESS STEEL BAG FLAWS

TEST PIECE 12–10 PLY BORON PREPREG AND ALUMINUM

HORN DRIVE

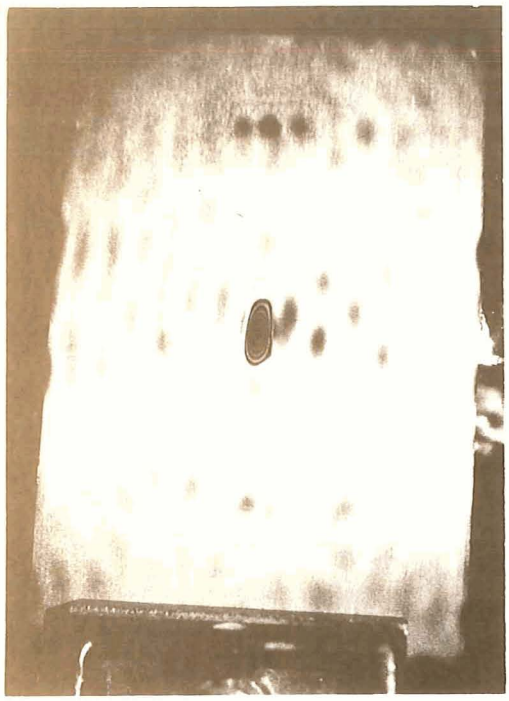

(a) 52 KHz RELATIVE AMPLITUDE 1

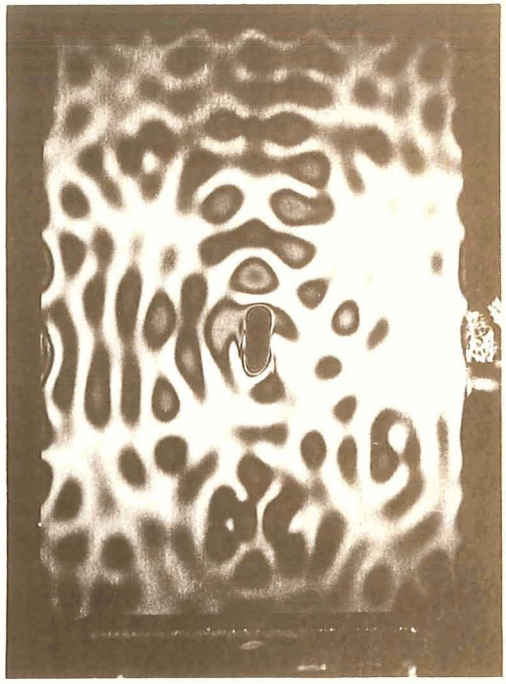

(b) 52 KHz RELATIVE AMPLITUDE 2

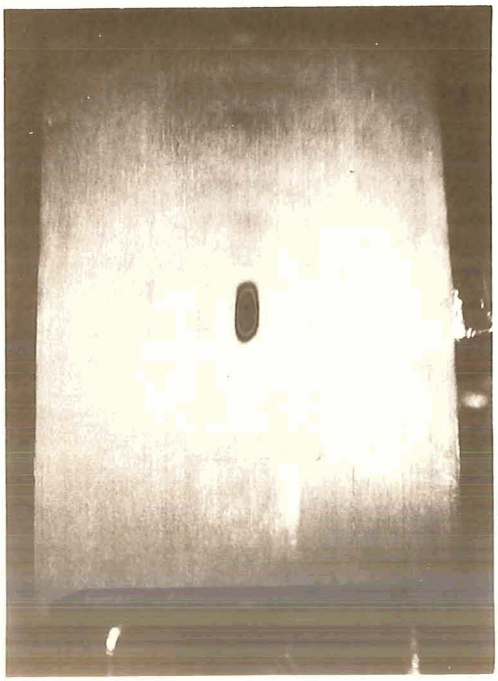

(c) 52.5 KHz MINIMUM PLATE MODE

FIG. 15

COMPOSITE BOND INSPECTION

STAINLESS STEEL BAG FLAWS

NASA FLAW SAMPLE – BORON PREPREG AND TITANIUM

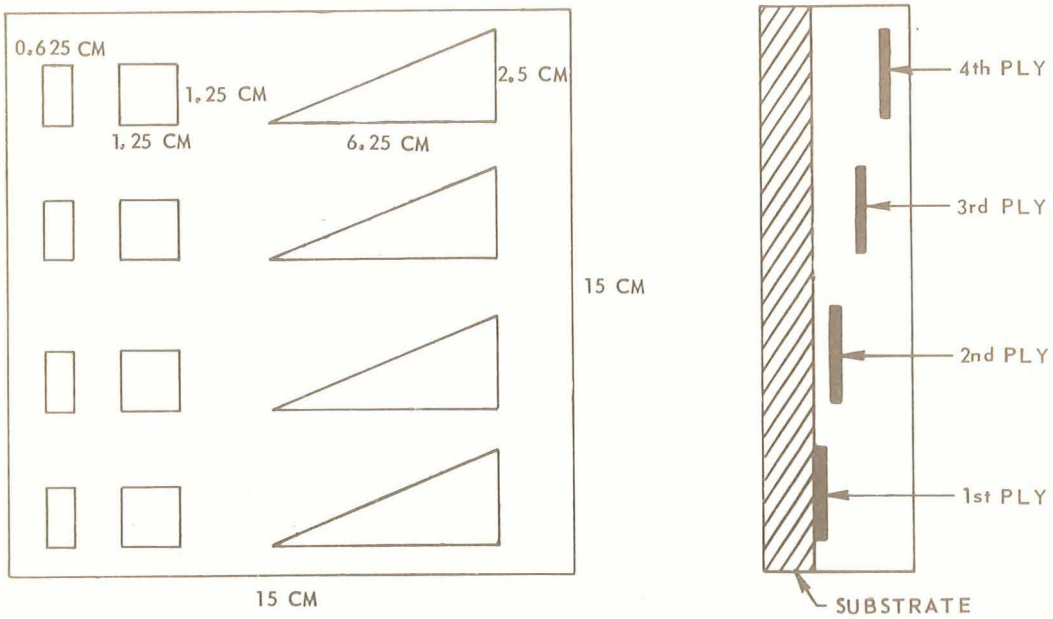

(a) FLAW LOCATION

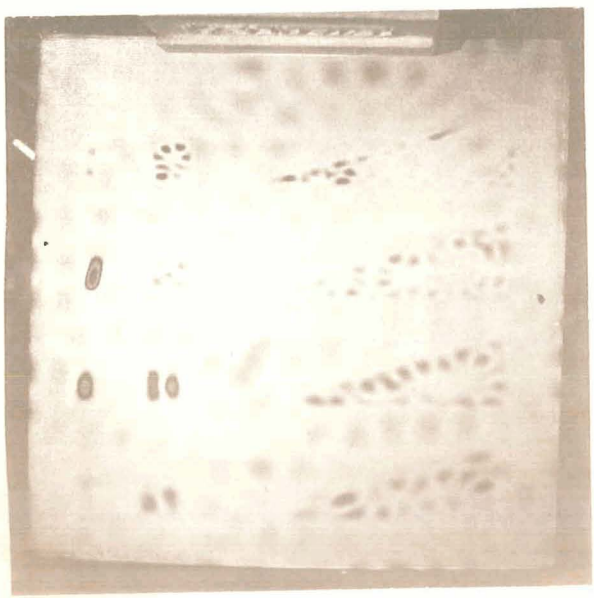

(b) HOLOGRAPHIC RECONSTRUCTION 52 KHz

COMPOSITE BOND INSPECTION

REAL TIME HOLOGRAPHIC OBSERVATION PHOTOGRAPHS
THERMAL STRESSING – BORON EPOXY PREPREG AND ALUMINUM
TEFLON TRIANGULAR FLAW.

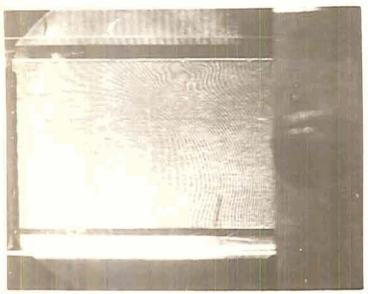

(5 SEC)

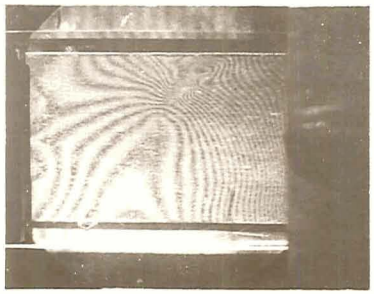

(5 MIN)

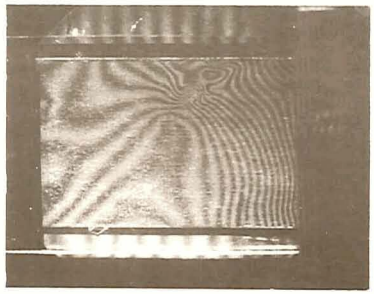

(10 MIN)

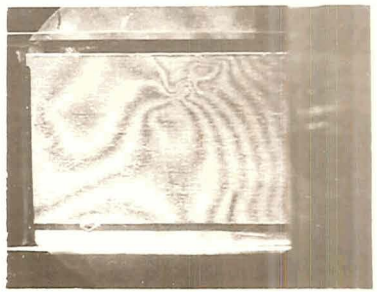

(15 MIN)

ELAPSED TIME AFTER THERMAL STRESSING

FIG. 16

COMPOSITE BOND INSPECTION
IR SCANNING CAMERA THERMOGRAMS

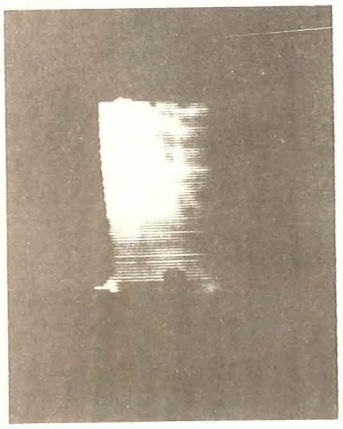

IR SCAN

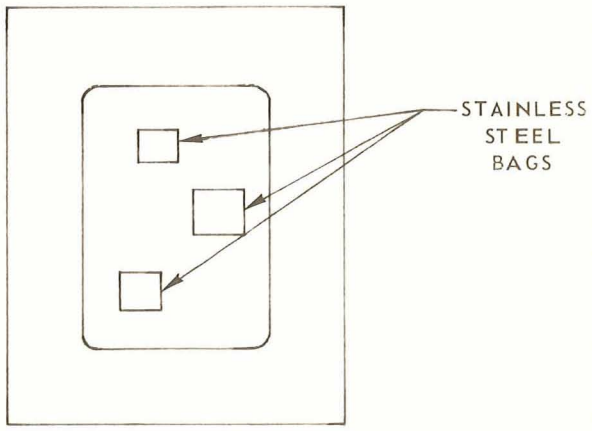

FLAW POSITIONS

TEST PIECE 4

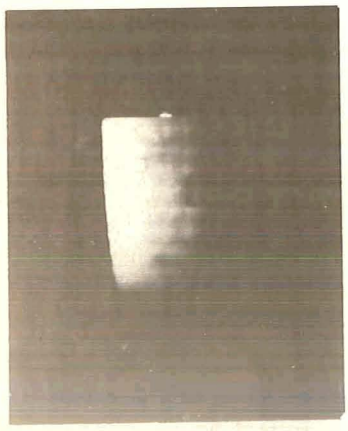

IR SCAN

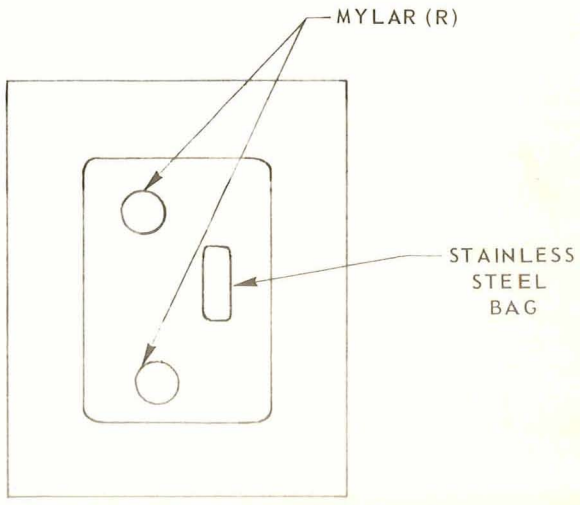

FLAW POSITIONS

TEST PIECE 5

FIG. 18

COMPOSITE BOND INSPECTION

IR SCANNING CAMERA THERMOGRAMS

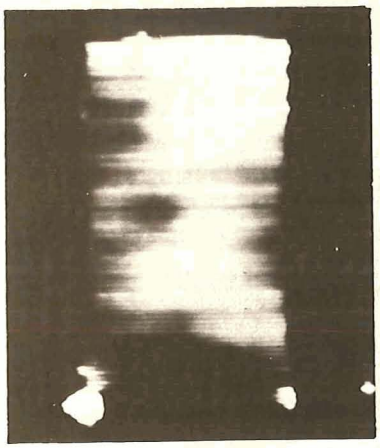

IR SCAN

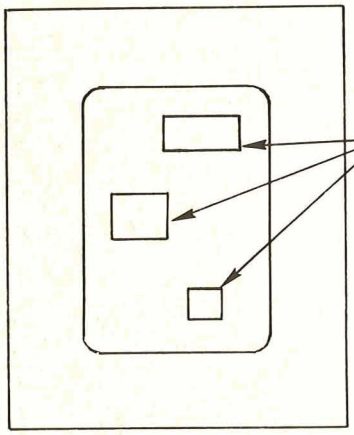

FLAW POSITIONS

TEST PIECE 7

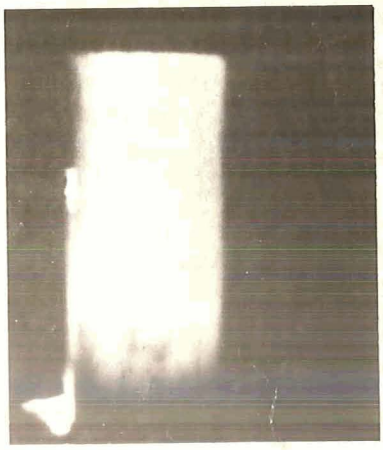

IR SCAN

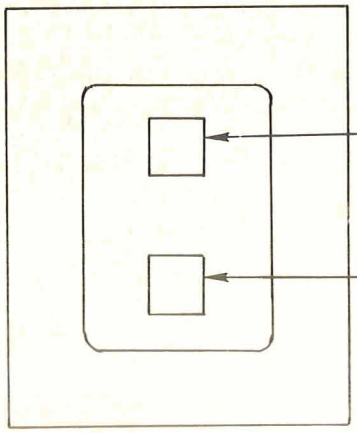

FLAW POSITIONS

TEST PIECE 8